Copy No._____

Defence Research and Development Canada
Recherche et développement pour la défense Canada

DEFENCE R&D DÉFENSE

Broadband pulse synthesis with the high frequency Multi-Mode Pipe Projector

J. Fawcett
J. Sildam
T. Miller
R. Fleming
M. Trevorrow

Defence R&D Canada – Atlantic

Technical Memorandum
DRDC Atlantic TM 2005-022
April 2005

Canada

This page intentionally left blank.

Broadband pulse synthesis with the high frequency Multi-Mode Pipe Projector

J. Fawcett

J. Sildam

T. Miller

R. Fleming

M. Trevorrow

Defence Research & Development Canada Atlantic

Technical Memorandum

DRDC Atlantic TM 2005–022

April 2005

Author

Approved by

Ron Kuwahara
Head/Signatures

Approved for release by

for/ Kirk Foster
Chair/Document Review Panel

© Her Majesty the Queen as represented by the Minister of National Defence, 2005
© Sa majesté la reine, représentée par le ministre de la Défense nationale, 2005

Abstract

In this report we describe experiments carried out at the DRDC Atlantic tank facility with the high frequency broadband Multi-Mode Pipe Projector (MMPP). In particular, we examine the fidelity with which one can produce specified broadband pulses with and without compensation for the transducer's spectral characteristics. It is shown that extended pulses or pulse sequences can be accurately produced and that matched filtering very effectively compresses the time series in the case of extended pulses. In addition, the vertical beampattern of the transducers is discussed and the results of some experiments with 2 transducers are also presented.

Résumé

Le présent rapport comprend la description d'expériences effectuées dans le réservoir acoustique de RDDC Atlantique en utilisant le projecteur à tube multimode (MMPP pour Multi-Mode Pipe Projector) haute fréquence à large bande. En particulier, la fidélité avec laquelle on peut reproduire des impulsions à large bande spécifiées en compensant, et sans compenser, pour les caractéristiques spectrales du transducteur est examinée. Les impulsions sont générées, et le filtrage adapté permet de comprimer de façon très efficace la série chronologique des impulsions de durée prolongée. Le rapport comporte également une discussion du diagramme de faisceau vertical des transducteurs et les résultats de certaines expériences effectuées avec deux transducteurs.

This page intentionally left blank.

Executive summary

BACKGROUND

This is the first report in a series of reports dealing with aspects of the TIF project "Exploiting Ultra-Wideband and Coded Sonar Pulses". In this report we investigate the characteristics and potential of the smallest of the Multi-Mode Pipe Projector (MMPP) transducers which has a useful frequency range from about 20-120 kHz. This very wide bandwidth allows the transducer to accurately create either very short duration pulses or complicated extended pulses such as Chirps or sequences of smaller pulses. It is hoped that the wideband capabilities of the MMPP technology will be useful in a variety of applications such as underwater communications, decoy signals, low amplitude extended sonar pulses, and target scattering. These applications have naval relevance for improved mine classification, stealthy underwater communication, torpedo jamming, and diver detection systems.

SIGNIFICANCE OF RESULTS

It is shown that the high frequency MMPP transducer has a wide frequency bandwidth. The spectral characteristics of the transducer can be compensated for in the construction of the waveform input to the transducer. The resulting output waveform accurately replicates the desired waveform. Matched filtering techniques can be effectively applied to the time series recorded from the transducer to increase the signal to noise ratio and to temporally compress the received waveform. The beampattern (horizontal and vertical) characteristics of the transducer vary significantly with the orientation of the transducer and for different applications, it may be advantageous to vary the orientation of the transducer. The characteristics of the transducer, as described in this report, indicate that it may be useful for a variety of important naval applications such as underwater communications, torpedo decoy signals, diver detection systems, and mine classification.

FUTURE WORK

There is much work remaining with the use of the MMPP transducers. The characteristics of the other 2 sized transducers will be investigated. As well, the use of these transducers in conjunction with each other to increase and flatten the overall spectral response will also be investigated. The application of these transducers and possibly arrays of these transducers will be investigated in more realistic, longer range sea trials.

Fawcett, J., Sildam, J., Miller, T., Fleming, R., and Trevorrow, M., 2005. Broadband pulse synthesis with the high frequency Multi-Mode Pipe Projector. DRDC Atlantic TM 2004-272, Defence R&D Canada - Atlantic.

Sommaire

INTRODUCTION

Le présent rapport est le premier d'une série de rapports qui vont traiter de divers aspects du projet FIT portant sur l'utilisation d'impulsions sonar à bande ultra-large et des impulsions sonar codées (Exploiting Ultra-Wideband and Coded Sonar Pulses). Des travaux de recherche sur les caractéristiques et le potentiel du plus petit des transducteurs MMPP, dont la plage de fréquences utiles s'étend d'environ 20 à 120 kHz, sont décrits dans le présent rapport. Cette largeur de bande étendue permet au transducteur de créer avec précision soit des impulsions de très courte durée, soit des impulsions complexes de durée prolongée, comme des ondes entretenues modulées en fréquence (chirps) ou des séquences d'impulsions plus courtes. On espère que les capacités large bande de la technologie MMPP seront utiles pour de nombreuses applications, dont les télécommunications sous-marines, les signaux de leurre, les impulsions sonar de durée prolongée à faible amplitude, et la dispersion par la cible. Ces applications présentent un intérêt pour la marine en ce qui à trait à la classification améliorée des mines, aux télécommunications sous-marines indétectables, aux systèmes de brouillage visant les torpilles, et aux systèmes de détection de plongeurs.

PORTÉE

Il est démontré que le transducteur MMPP haute fréquence a une grande largeur de bande. On peut compenser pour les caractéristiques spectrales du transducteur par la génération de formes d'onde d'entrée au transducteur. La forme d'onde de sortie résultante correspond avec précision à la forme d'onde désirée. Des techniques de filtrage adapté peuvent être appliquées efficacement à la série chronologique enregistrée à partir du transducteur afin d'augmenter le rapport signal sur bruit et de comprimer temporairement la forme d'onde reçue. Les caractéristiques des diagrammes de faisceau (horizontal et vertical) du transducteur varient de façon significative en fonction de son orientation. Pour différentes applications, il peut donc être avantageux de modifier l'orientation du transducteur. Les caractéristiques du transducteur, décrites dans le présent rapport, indiquent que cela pourrait être utile dans le cas de nombreuses applications importantes pour la marine, comme les télécommunications sous-marines, les signaux de leurre visant les torpilles, les systèmes de détection de plongeurs et la classification des mines.

RECHERCHES FUTURES

Il reste encore beaucoup de travail à faire en ce qui a trait à l'utilisation des

transducteurs MMPP. On compte faire des recherches sur les caractéristiques des deux autres transducteurs, ainsi que sur l'utilisation combinée de ces transducteurs afin d'augmenter et d'aplatir la réponse spectrale globale. De plus, l'utilisation de ces transducteurs et, possiblement, de réseaux de transducteurs fera l'objet d'essais en mer sur des plus grandes distances, dans un environnement plus réaliste.

Table of contents

Abstract i

Résumé i

Executive summary iii

Sommaire iv

Table of contents vi

List of figures vii

Acknowledgements x

1 INTRODUCTION 1

2 PULSE EXPERIMENTS 2

2.1 Pulse types 2

2.2 Frequency response measurements 2

2.3 Uncompensated and compensated time series 7

2.4 Some Matched Filtering Results 15

3 VERTICAL BEAMPATTERN 25

4 DISCUSSION OF RESULTS 28

References 30

Distribution List 31

List of figures

1 Transmit voltage response (dB re 1 μ Pa/Volt @ 1m) curves for the MMPP transducer at 1.83 m (approx. 6 feet) depth 3

2 The spectral response of the MMPP (HF) transducer (z-axis) as a function of the centre frequency of the 80-kHz constant bandwidth signal 4

3 The spectral response of the MMPP (HF) transducer for the centre frequency of 50 kHz and bandwidth of 80 kHz. 5

4 Two MMPP transducers vertically aligned 5

5 The spectral responses of 2 MMPP (HF) transducers as a function of the centre frequency of the 80-kHz constant bandwidth signal for [top row] transducers wired in series, out-of-phase, in-phase [bottom row] in parallel, out-of-phase, in-phase 6

6 The spectral responses of a single MMPP (HF) transducer (blue) and 2-transducer system (parallel, out-of-phase) (red) for the centre frequency of 40 kHz and bandwidth of 80 kHz. 6

7 The spectral responses of a single MMPP (HF) transducer (blue) and 2-transducer system (parallel, out-of-phase) (red) for the centre frequency of 80 kHz and bandwidth of 80 kHz. 7

8 The resulting power spectrum (dB) for 20-kHz bandwidth pulses centred, top to bottom, at 30,50,70, and 90 kHz respectively and the corresponding time series - red is the original input signal. Both the time series and spectra have been normalized to have a peak amplitude of unity 8

9 The recorded time series for an uncompensated Sinc pulse with a centre frequency of 75 kHz and a bandwidth of 80 kHz. 9

10 The experimental spectrum for an uncompensated Sinc pulse with a centre frequency of 75 kHz and a bandwidth of 80 kHz. . 10

11 The spectral amplitude of the compensating spectrum Q(f) . . . 11

12 The phase of the compensating spectrum Q(f) 11

13 The pre-compensated time series input to the waveform generator to produce a 80-kHz Sinc Function 12

14 The time series resulting from the input waveform of Fig. 13 - blue is time series, red is desired time series. The desired time series is shown at twice the hydrophone sampling rate. 13

15 The measured output spectrum corresponding to the pre-compensated 80-KHz bandwidth Sinc time series. 13

16 The time series resulting from the compensated waveform for a 60-kHz bandwidth Sinc pulse - blue is time series, red is desired time series. The desired time series is shown at twice the hydrophone sampling rate. 14

17 The spectrum corresponding to the output 60-KHz bandwidth Sinc time series. 14

18 The resulting Chirp time series (blue) with desired series superimposed in red - 80 kHz bandwidth 15

19 A zoom of the 80-kHz bandwidth Chirp time series (blue) with desired series superimposed in red 16

20 The resulting Chirp time series (blue) with desired series superimposed in red - 60 kHz bandwidth 16

21 A zoom of the 60-kHz bandwidth Chirp time series (blue) with desired series superimposed in red 17

22 Computed time/frequency plot of experimental 80-kHz Chirp . . 17

23 Computed time/frequency plot of experimental 60-kHz Chirp . . 18

24 A 5 pulse Barker sequence using individual Gaussian pulses with a separation of 20 samples (80 μsecs) between pulses and 10 samples (40 μsecs) between pulses) 19

25 A 11 pulse Barker sequence using a cosine carrier at 62.5 kHz . . 20

26 The spectrum of the Barker code time series of Fig. 25 20

27 The matched filter time series using the Barker code of individual Gaussian pulses separated by 80 μsecs and 40 μsecs respectively) 21

28 The matched filter time series from the 11 Barker code using a 62.5 kHz cosine burst. 22

29 The small aluminum-shelled sphere that was deployed in tank . 22

30 The timeseries with overlapping incident and multipath pulses. . 23

31 The matched filtered version of the time series of Fig. 30 24

32 The matched filtered version of the time series of Fig. 30, zoomed in near the region of the sphere echo 24

33 The vertical beampattern of the transducer for an uncompensated 80-kHz Sinc waveform 26

34 The vertical beampattern of the transducer for a compensated 80-kHz Sinc waveform for the broadside direction 26

35 Time series using compensated Sinc pulse (20-70 kHz) for transducer endcap facing hydrophone 27

36 The power spectrum of the resultant signal 27

Acknowledgements

We would like to thank Sean Spears, Mark Rowsome, and Chris Purcell for their help in various aspects of our experiments. Also, discussions with Brian Maranda regarding aspects of the signal processing were very useful.

1 INTRODUCTION

In 2003 TIF funding was granted for the project "Exploiting Ultra-Wide-Band and Coded Sonar Pulses". This project proposed using the transducer technology, Multi-Mode Pipe Projector (MMPP), developed at DRDC Atlantic [1,2] as the type of transducer for the study of various wideband applications. In particular, 3 different MMPP sizes will be considered during this TIF project. For the studies in this report, we focus on the smallest transducer which has significant output in the frequency range 20-120 kHz. The dimensions of the transducer are approximately, 5.3 cm high and a diameter of 3.7 cm. The small size of this transducer means that it should be straightforward to construct systems with arrays of these transducers.

The concept of the MMPP is based upon synthesizing a wideband output for a transducer by constructing a transducer with a set of many resonances spread across the frequency spectrum. This results in a significant power output over the entire band of frequencies spanned by the resonances of the system. It also means, however, that the resulting power spectrum for the transducer is not flat as there are peaks and nulls resulting from the combined response of the resonances of the system. Thus, it is not clear with what fidelity one can reproduce specific pulse types. For some sonar applications, it may not be very important to be able to reproduce exactly specified pulses - it may be sufficient to simply use the pulse output by the transducer. However, for applications such as producing realistic decoy signals, it is clearly important to be able to accurately reproduce specified signals.

In the first part of Section 2.2 we show the transducer response for constant bandwidth signals (Sinc functions in the time domain) as a function of the centre frequency and bandwidth for a single transducer. We also show the responses for 2 transducers mounted vertically and wired in series, with reversed and the same polarities and wired in parallel with reversed and the same polarity.

With a knowledge of the power spectrum output of the transducer over a given bandwidth, we can attempt to design a compensated input pulse which yields the desired output pulse. The results of this process will be presented for both narrow and extended pulses. As well, the result of match-filtering the recorded time series will be presented. Finally, the vertical beampattern of the transducer will be investigated and the significance of the beampattern discussed.

2 PULSE EXPERIMENTS

2.1 Pulse types

In this section we describe the main pulse types we use in the tank experiments. First, we consider a constant bandwidth pulse with centre frequency f_c and bandwidth B_f. In the time domain the pulse is given by

$$S_s(t) = \frac{sin(2\pi B_f t/2)}{\pi B_f t} \cos(2\pi f_c t) \tag{1}$$

For very small bandwidths the signal is harmonic in nature with frequency f_c, for larger bandwidths the pulses becomes shorter and contain only a few cycles of the harmonic signal. A similar signal is obtained by considering a Gaussian distribution in the frequency domain (and its image for the negative frequencies),

$$S_g(t) = \cos(2\pi f_c t) \exp(-2\pi^2 \sigma_f^2 t^2) \tag{2}$$

where σ_f is the standard deviation of the pulse in the frequency domain. For extended pulses we use the CHIRP subroutine of the signal processing toolbox in MATLAB. Here the instantaneous frequency of the pulse will vary linearly from a specified f_0 at $t = 0$ to f_1 at a specified end time (we will use one millisecond).

2.2 Frequency response measurements

The experiments we describe in this report took place in the DRDC Atlantic acoustic calibration tank. The high-frequency MMPP was deployed at a depth of 1.83 m and a B&K 8100 calibrated hydrophone was deployed 2 m away. In Fig.1 we show the Transmit Voltage Response curves obtained for the 5 different high frequency MMPP transducers using the standard DRDC Atlantic calibration acquisition and software suite. As can be seen the 5 curves are very similar except for a deeper null in one curve in the region of 80 kHz. There are significant vertical beampattern effects at the high frequencies and the difference here may be due to a slight change in the geometry or relative orientation of the transducer. However, there is certainly a null in the responses of all 5 transducers at approximately 30 and 80 kHz.

A data acquisition and waveform generation program was written in LABVIEW which allowed for the sequential generation of Sinc and Gaussian pulses as a function of centre frequency and bandwidth (with a specified σ_f in the case of the Gaussian pulses) and for the recording of the resulting signals at

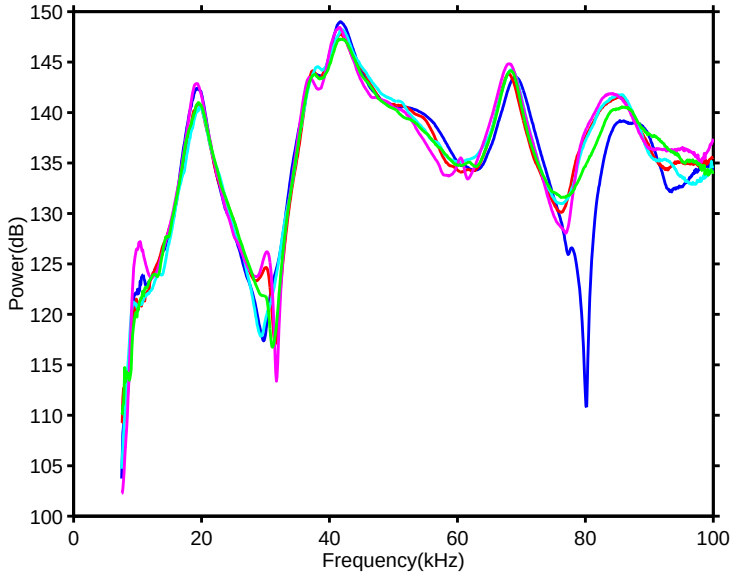

Figure 1: *Transmit voltage response (dB re* $1\ \mu\ Pa/Volt$ *@ 1m) curves for the MMPP transducer at 1.83 m (approx. 6 feet) depth*

the hydrophone. For the data of this report, the time series was sampled at 250000 samples/second. As well, text files of arbitrary waveforms can be used by the LABVIEW program.

In order to test transducer linearity, a series of tests with wideband pulses were conducted. In Fig. 2 we show a two-dimensional image of the resulting power spectra, computed by a MATLAB program, as the centre frequency f_c of a Sinc pulse is varied from 10 to 100 kHz in steps of 200 Hz for a bandwidth of 80 kHz. The x-coordinate is the centre frequency of the Sinc pulse in kHz and the z-coordinate is the frequency axis for the computed FFT-power spectra. As can be seen, the input Sinc functions do not excite energy in the band outside the 80 kHz band width. Another encouraging feature is that at a given frequency value for the spectral response, the value is essentially independent of the centre frequency f_c (as long as it lies within the $\pm$ 40 kHz of the centre frequency). A somewhat unusual feature is the apparent folding of energy at the upper left and lower right corners of the plot. For the case of the low frequencies this is due to the fact that some of the frequency response centred about the negative value of the centre frequency appears in the positive spectrum. The effect in the lower right is due to spectral aliasing. In Fig. 3 the spectrum for a centre frequency of 50 kHz and total bandwidth of 80 kHz is shown. As can be seen this spectrum is very similar to the calibration spectra of Fig. 1. Thus, it seems that the transducer is exhibiting predictable linear behaviour.

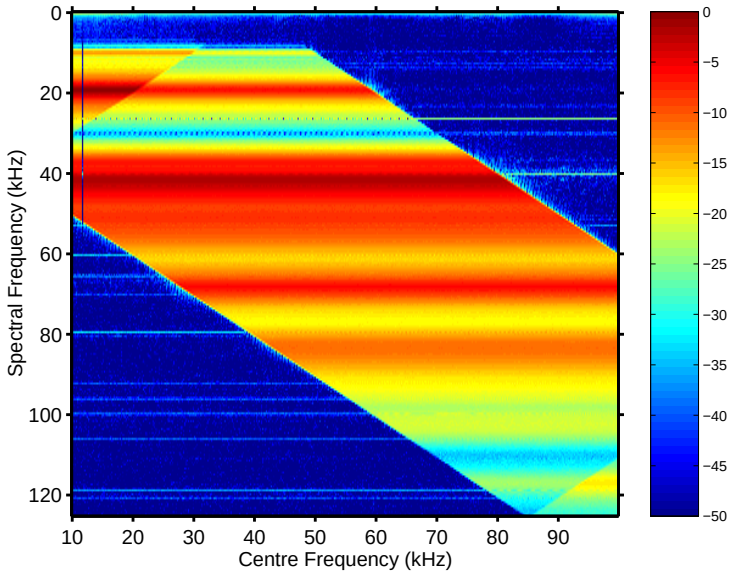

Figure 2: *The spectral response of the MMPP (HF) transducer (z-axis) as a function of the centre frequency of the 80-kHz constant bandwidth signal*

Due to the small size of the high-frequency MMPP, it is straightforward to form arrays of these transducers. In Fig. 4 a 2 element vertical array with a rigid connection of approximately 4 cm spacing is shown. These 2 transducers can be wired in series or in parallel and they can transmit in or out of phase with each other. In Fig. 5 we show the two-dimensional spectral response for the 4 possible arrangements. In this plot, the top row are the two transducers wired in series, out-of-phase and in-phase. The second row shows the results for the transducers wired in parallel. It is important to note that these results have all been normalized by their maximum amplitude and thus these plots do not indicate the absolute levels of the system output. In Figs.6 and 7 we compare the spectra from the single transducer (blue) and the two-transducer system (parallel, out-of-phase) (red) for centre frequencies of 40 and 80 kHz.

As can be seen, the use of 2 transducers, particularly when used out-of-phase has a noticeable effect. In Figs.6 and 7 the resulting frequency response for the two-transducer system is flatter at the high frequencies of 100 kHz and beyond and also in Fig.7 it can be seen that the null at 30 kHz has been somewhat shifted to a lower frequency. Thus it maybe possible to shape the spectral response by using more than one of these transducers together. It might be useful in the future to investigate more thoroughly the effects of combining the individual transducers and the effect of the spacing distance between them.

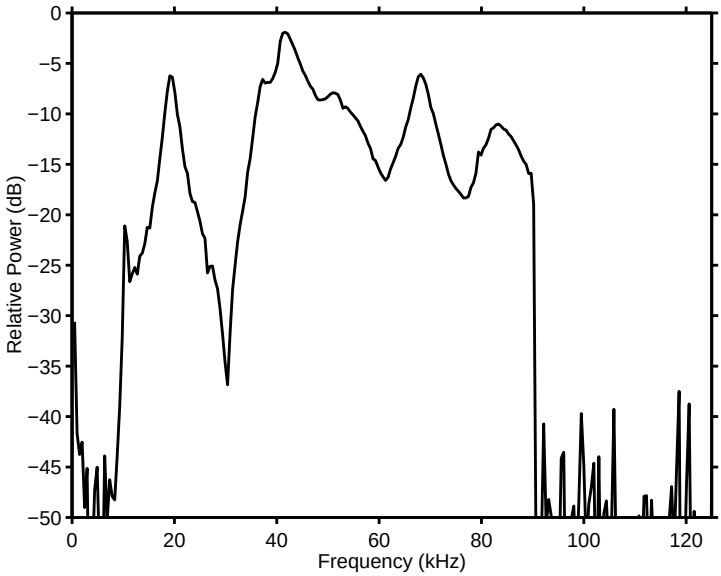

Figure 3: *The spectral response of the MMPP (HF) transducer for the centre frequency of 50 kHz and bandwidth of 80 kHz.*

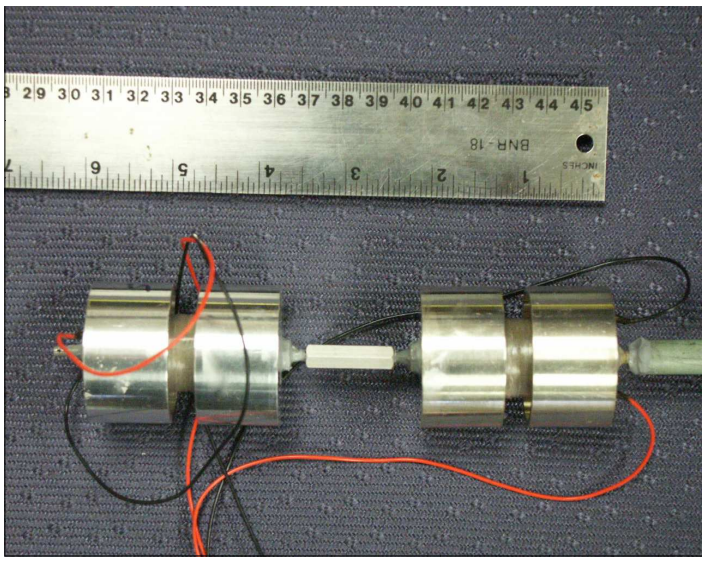

Figure 4: *Two MMPP transducers vertically aligned*

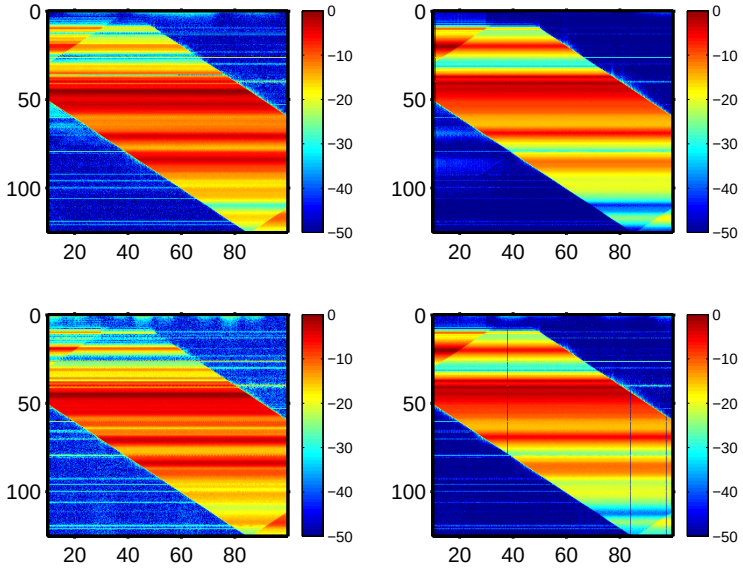

Figure 5: *The spectral responses of 2 MMPP (HF) transducers as a function of the centre frequency of the 80-kHz constant bandwidth signal for [top row] transducers wired in series, out-of-phase, in-phase [bottom row] in parallel, out-of-phase, in-phase*

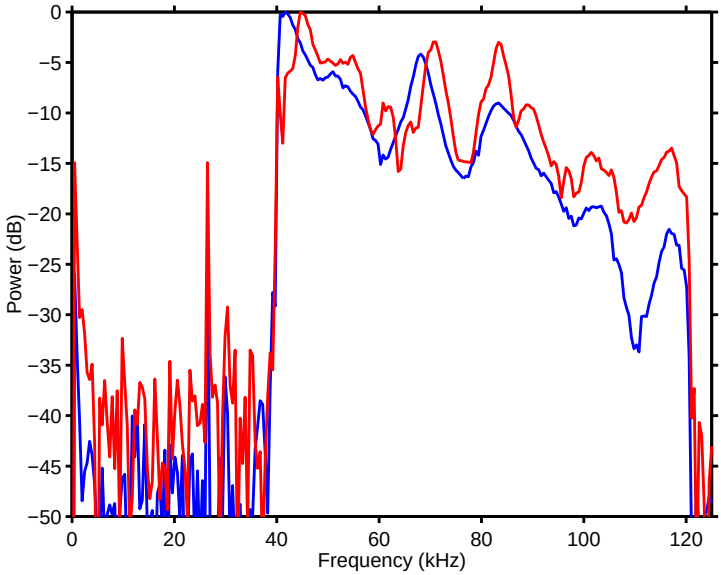

Figure 6: *The spectral responses of a single MMPP (HF) transducer (blue) and 2-transducer system (parallel, out-of-phase) (red) for the centre frequency of 40 kHz and bandwidth of 80 kHz.*

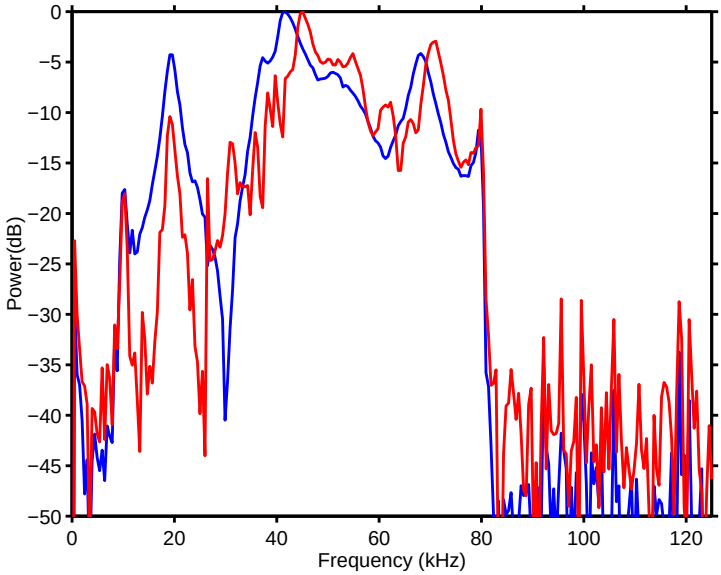

Figure 7: *The spectral responses of a single MMPP (HF) transducer (blue) and 2-transducer system (parallel, out-of-phase) (red) for the centre frequency of 80 kHz and bandwidth of 80 kHz.*

2.3 Uncompensated and compensated time series

In this section we first show in Fig.8 some of the spectra and time series for 20 kHz bandwidth Sinc pulses with centre frequencies of 30, 50, 70, and 90 kHz. As well we superimpose the desired Sinc pulse on the experimental time series. The location of the theoretical pulse is determined by finding the time shift which maximizes the cross-correlation of the theoretical pulses with the recorded signal. There is no physical interpretation as to this location; it is simply the location which mathematically produces the largest correlation. As is seen in Fig. 8 the resulting matches between the theoretical and the recorded time series are not, in general, good for these uncompensated input waveforms. It is clear from the results of Fig. 8 that the output spectra resulting from a constant input spectra (across the specified bandwidth) are far from flat. This is not surprising considering the spectral response of the transducer as shown in Fig. 1. In the top spectral plot of Fig. 8 there is no apparent energy at 30 kHz even though the Sinc pulse is centred at 30 kHz. This is due to the fact, as seen in Fig. 7, that there is a significant null at approximately 30 kHz. From the relative flatness of the spectrum, we would expect to obtain the best uncompensated pulses for centre frequencies in the range of approximately 40-60 kHz and indeed the response at 50 kHz, the second plot of Fig. 8, is the closest to the desired output.

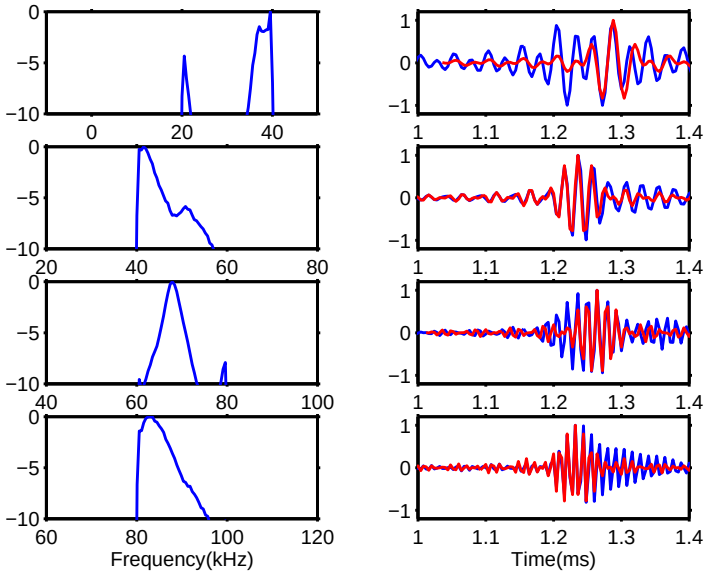

Figure 8: *The resulting power spectrum (dB) for 20-kHz bandwidth pulses centred, top to bottom, at 30,50,70, and 90 kHz respectively and the corresponding time series - red is the original input signal. Both the time series and spectra have been normalized to have a peak amplitude of unity*

By considering the complex-valued (i.e., both amplitude and phase) spectral response of the transducer to a given input waveform, we can compute the transfer function to apply to a waveform in order to produce that waveform at the output of the transducer. Letting $S(f)$ be the recorded output spectrum, $T(f)$ the transfer function of the transducer, and $B(f)$ the original input spectrum, then one can write

$$S(f) = T(f)B(f) \tag{3}$$

Let us define

$$Q(f) = 1/T(f) = \frac{B(f)}{S(f)}. \tag{4}$$

From Eq.(3), it is easy to show that if the waveform corresponding to the spectrum $Q(f)B(f)$ is input then the waveform output from the transducer will correspond to $B(f)$. In practice, as $S(f)$ becomes relatively small in amplitude (for example, with respect to the background noise spectrum) the division in Eq.(4) may become unstable. Thus we use the following formula for $Q(f)$ after $S(f)$ has been normalized to have a maximum amplitude of

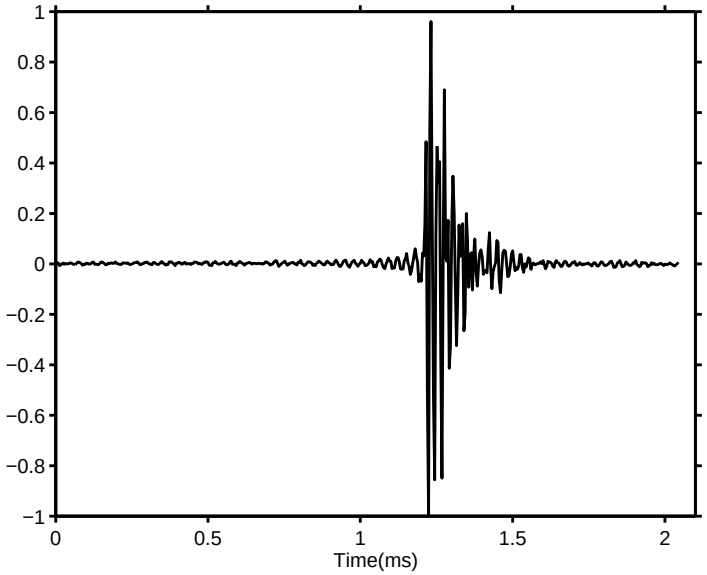

Figure 9: *The recorded time series for an uncompensated Sinc pulse with a centre frequency of 75 kHz and a bandwidth of 80 kHz.*

unity,

$$Q(f) = \frac{B(f)}{S(f)/|S(f)|(|S(f)| + a)} \tag{5}$$

where a is a scalar which we set to 0.05 in the examples below. The compensating spectrum $Q(f)$ can be used for any desired spectrum $\tilde{B}(f)$ which is contained within the same frequency bandwidth as $B(f)$. It should be noted that in this report we use a spectral compensation approach. It is possible to construct a finite time series from $Q(f)$ and perform the compensation in the time domain by a convolution. For some applications this could be preferable.

As an example of the spectral compensation of an input waveform, let us consider the 80-kHz bandwidth response to the pulse with a centre frequency of 75 kHz. The recorded resulting pulse is shown in Fig. 9 and its spectrum in Fig. 10. It is clear from Fig.9 that the output waveform is far from the very sharp pulse which should result from this bandwidth and it is clear from Fig. 10 that the spectral response is far from flat. Performing the operation of Eq.(5) we obtain the results shown in Fig. 11 for the amplitude of the compensation function $Q(f)$ and in Fig. 12 for the phase. For the phase of the spectrum of $Q(f)$, we first unwrapped the phase of the spectrum (using the MATLAB function UNWRAP) and then differenced the phase with respect to frequency to make the linear phase change (which can result simply from propagation or a time delay) a constant. As can be seen, the significant phase changes occur at approximately 60 and 80-kHz.

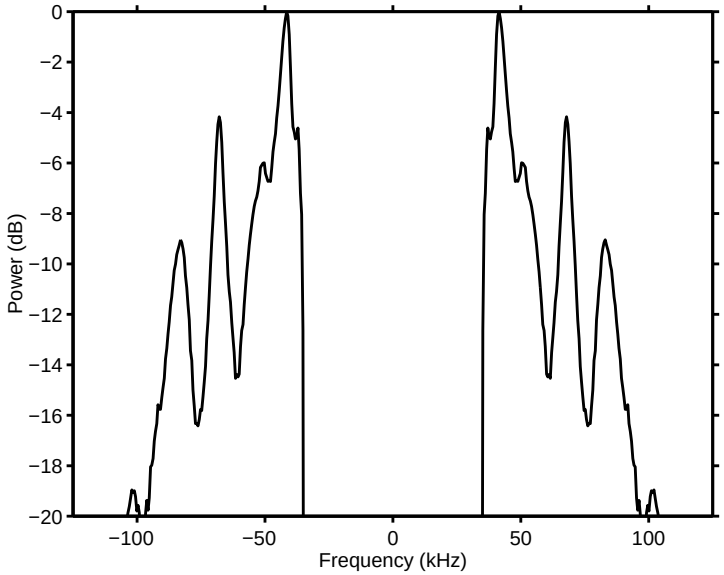

Figure 10: *The experimental spectrum for an uncompensated Sinc pulse with a centre frequency of 75 kHz and a bandwidth of 80 kHz.*

It is not clear what the resulting power loss to the output signal will be as a result of the spectral flattening. In the normalization of Eq.(5) the peak value of $S(f)$ is normalized to have unit amplitude so that the division effectively emphasizes the spectral components for frequencies other than the peak frequency. However, the time series which is supplied to the MMPP waveform generator is first normalized to have a peak amplitude of unity so that the absolute levels of the spectrum do not affect the compensated time series that is computed. However, by decreasing the relative contribution of frequencies (e.g., 40 kHz) and increasing the spectral amplitude of "inefficient" frequencies (e.g., 80 kHz) one would expect the transducer to produce less acoustic energy for a fixed amount of applied voltage. For example, the difference between the response at 42 kHz to that at approximately 78 kHz is about 15 dB. The linear amplitude reduction for the 42 kHz response corresponding to a 7.5 dB drop (i.e., the output at 42 kHz is decreased by 7.5 dB and the ouput at 78 kHz increased by the same amount) is 0.421. The overall output levels can be increased by increasing the voltage applied to the system and thus, in practice, the levels which can be obtained with the spectrally-flattened signal will depend upon the maximum voltage levels which can be applied to the transducer.

In Fig. 13 we show the compensated signal used by the MMPP for the 80-kHz Sinc pulse (35 kHz $\leq f \leq$ 115 kHz). It is clearly significantly different than the desired Sinc pulse. The resulting recorded signal (and the overlaid desired

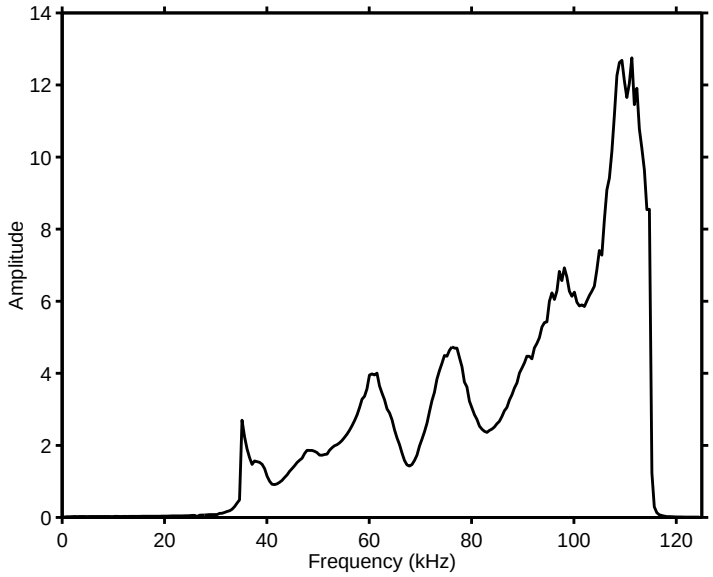

Figure 11: *The spectral amplitude of the compensating spectrum Q(f)*

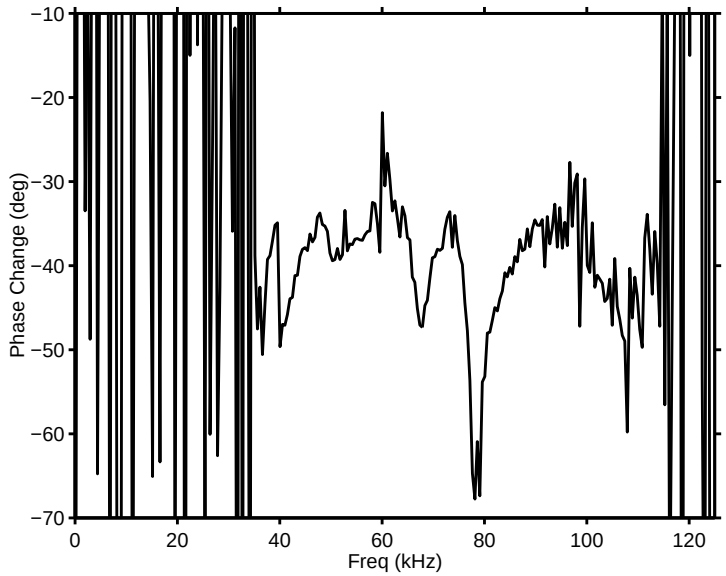

Figure 12: *The phase of the compensating spectrum Q(f)*

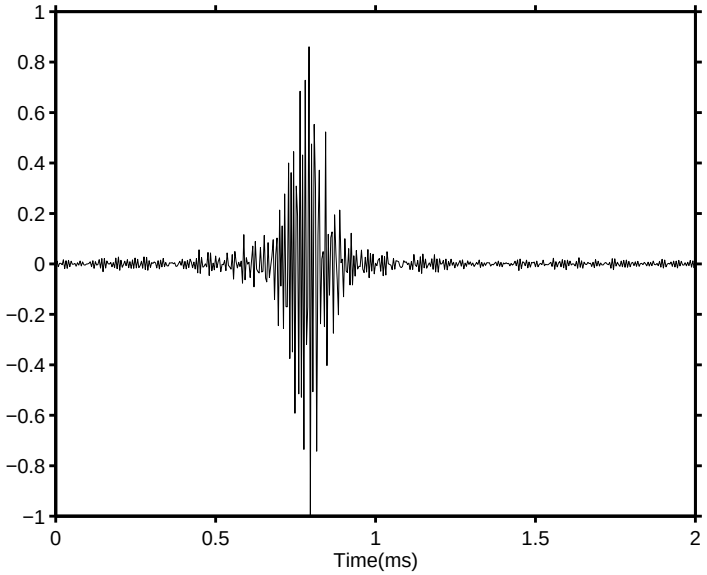

Figure 13: *The pre-compensated time series input to the waveform generator to produce a 80-kHz Sinc Function*

Sinc pulse) is shown in Fig. 14 and its spectrum in Fig. 15. From Fig. 14 it can be seen that the compensation was largely successful in producing the desired output waveform. Fig. 15 shows that the resulting spectrum is quite flat with the exception of frequencies greater than approximately 100 kHz where the relative levels are somewhat low. The lower levels are probably due to the use of the scalar floor a in the definition of $Q(f)$ in Eq.(4). In Fig. 16 and 17 we show the corresponding results for a 60-kHz bandwidth pulse centred at 65 kHz. From these figures, it can be seen that the agreement of the output pulses with the desired pulses is very good, particularly for the 60-kHz bandwidth.

Instead of these very short pulses, we can apply the same compensation to produce cosine-tapered Chirp pulses of 1 millisecond duration. Figures 18 and 19 show the resulting Chirp pulses with the desired Chirp pulses superimposed in red for a 80-kHz wide Chirp and in Figures 20 and 21 the corresponding results for the 60-kHz wide Chirp. Perhaps, more informative than these time series plots are the spectrograms obtained by using short-time Fourier Transforms over the received signal. The resulting time/frequency plots are shown in Figs. 22 and 23. As can be seen the spectograms of the recorded signals exhibit the correct frequency/time variation. The second arrival which is evident in the plots is from the surface reflection. The vertical angle for this multipath is quite large, due to the short-range geometry used in the tank, and since the frequency response of the transducer at this vertical angle is quite different than that at horizontal, the surface reflection is not simply an

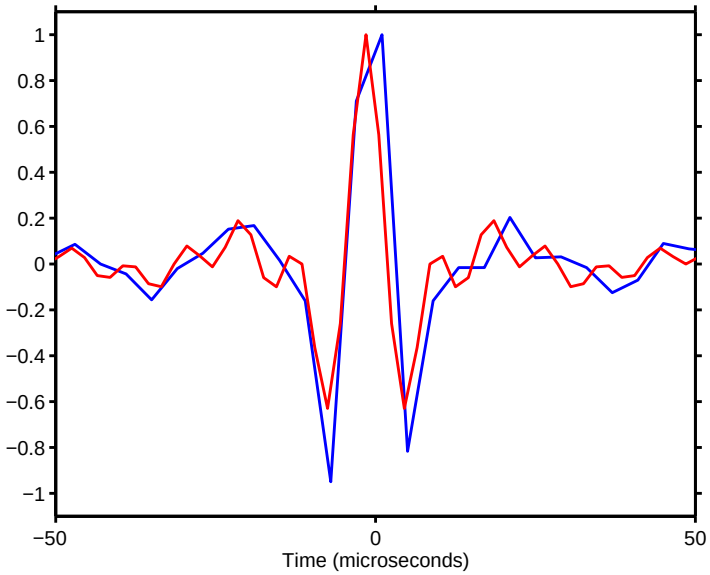

Figure 14: *The time series resulting from the input waveform of Fig. 13 - blue is time series, red is desired time series. The desired time series is shown at twice the hydrophone sampling rate.*

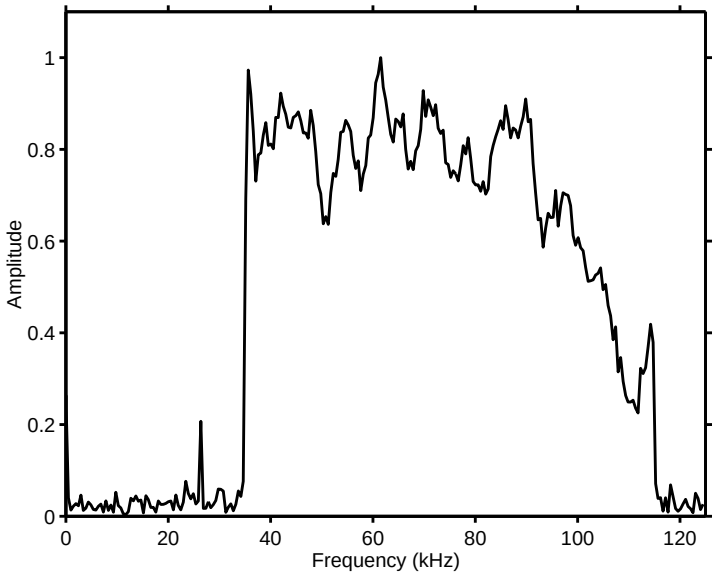

Figure 15: *The measured output spectrum corresponding to the pre-compensated 80-KHz bandwidth Sinc time series.*

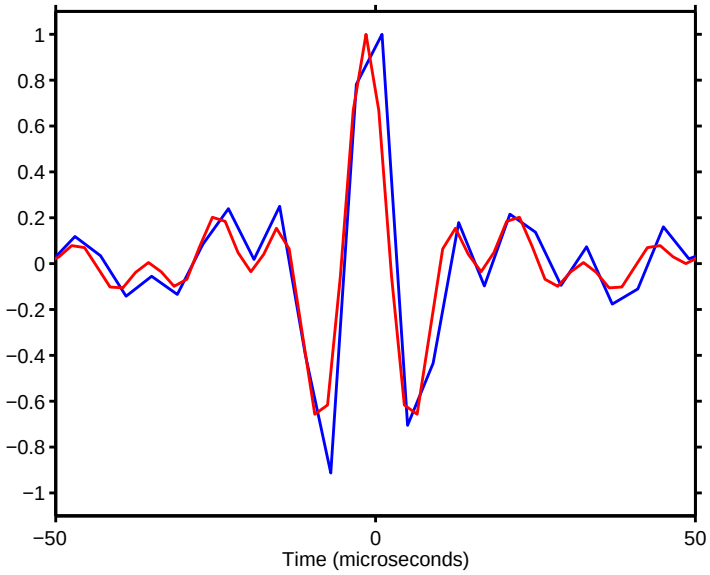

Figure 16: *The time series resulting from the compensated waveform for a 60-kHz bandwidth Sinc pulse - blue is time series, red is desired time series. The desired time series is shown at twice the hydrophone sampling rate.*

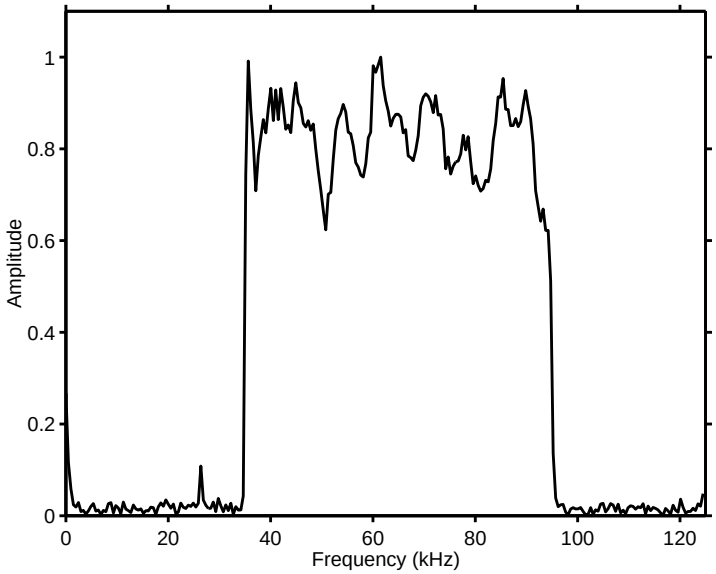

Figure 17: *The spectrum corresponding to the output 60-KHz bandwidth Sinc time series.*

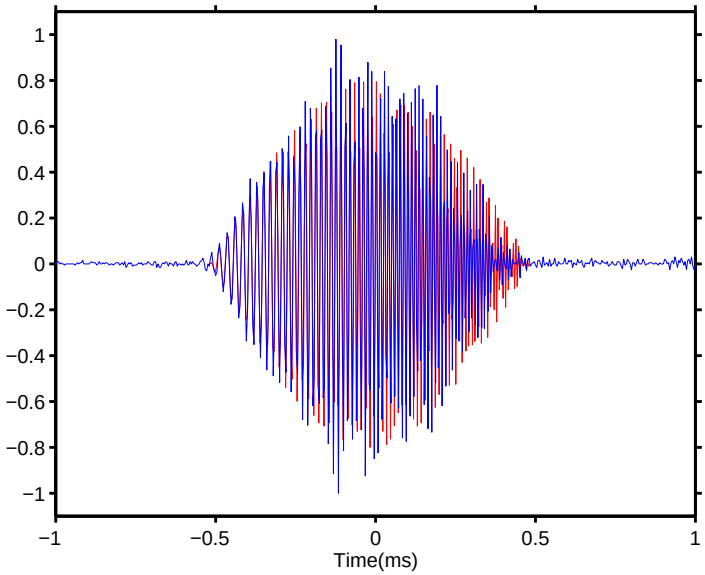

Figure 18: *The resulting Chirp time series (blue) with desired series superimposed in red - 80 kHz bandwidth*

inverted replica of the direct signal.

It is also possible to construct a pulse sequence by amplitude or phase modulating a basic pulse. For example, in Fig. 24 we show 2 5-pulse sequences (as recorded after compensation) constructed from a Gaussian pulse ($\sigma_f = 20$ kHz, centre frequency = 65 kHz) with positive and negative polarities. The difference between the 2 input pulse sequences used for Fig. 24 is the interpulse spacing: 80μsecs in the first case and 40μsecs in the second case. For this case we simply created the compensated time series by superimposing the compensated waveforms for the individual pulses. This sequence of ± 1 follows a Barker code [3] (1,1,1,-1,1). In Fig. 25 we show an 11-bit Barker Sequence (1,1,1,-1,-1,-1,1,-1,-1,1,-1) constructed from a sequence of 4-cycle 62.5 kHz pulses. The spectrum of the recorded Barker sequence of Fig. 25 is shown in Fig. 26. In Ref. 3 an application of these pulses to doppler sonars is presented.

2.4 Some Matched Filtering Results

When using extended pulses such as the one millisecond Chirps or the multipulse Barker Code sequences, it is anticipated that by match-filtering the time series the original extended pulses can be reduced to narrow peaks with respect to time in the matched filter domain. For example, in Fig. 27 we show the matched filter results (amplitude of the complex envelope formed using the

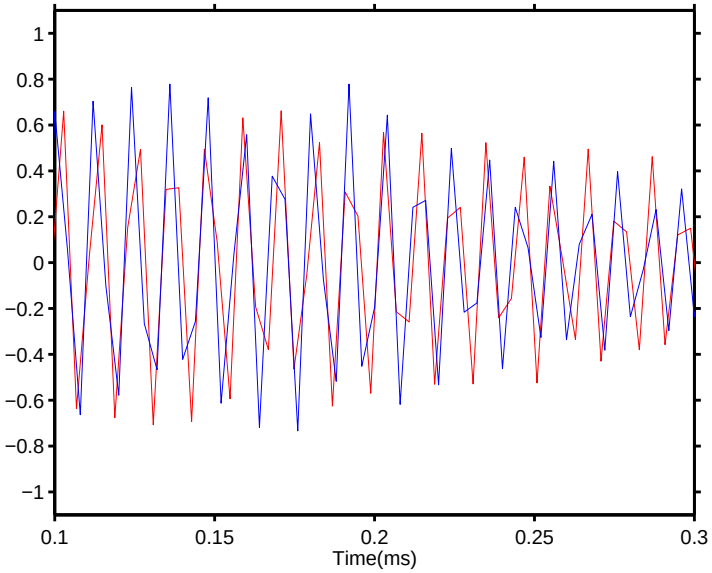

Figure 19: *A zoom of the 80-kHz bandwidth Chirp time series (blue) with desired series superimposed in red*

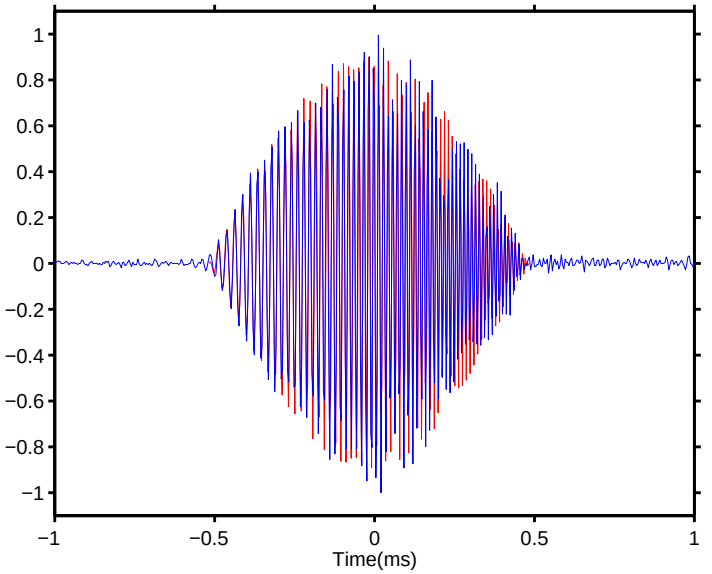

Figure 20: *The resulting Chirp time series (blue) with desired series superimposed in red - 60 kHz bandwidth*

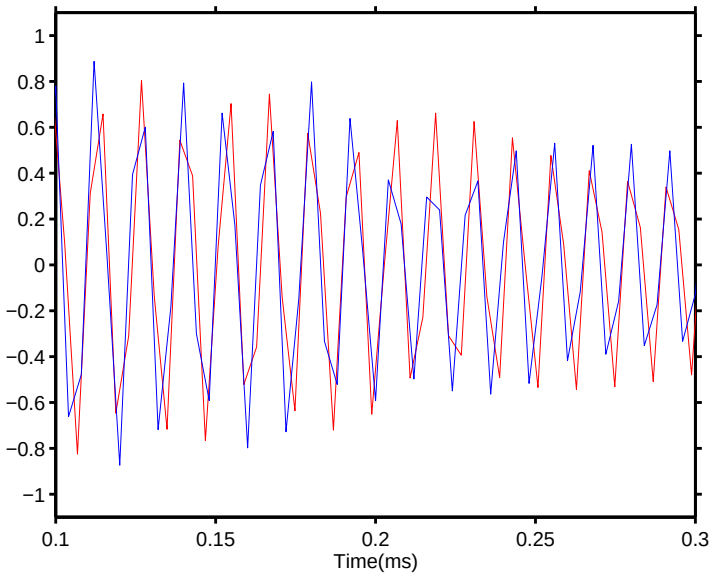

Figure 21: *A zoom of the 60-kHz bandwidth Chirp time series (blue) with desired series superimposed in red*

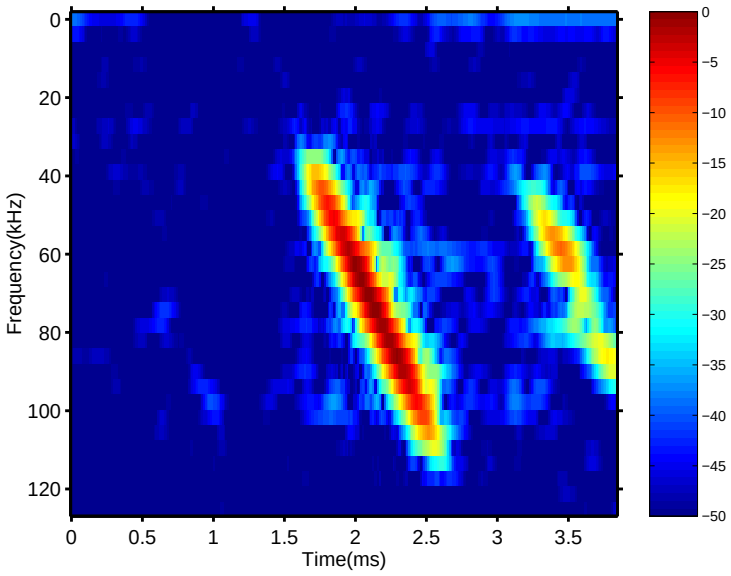

Figure 22: *Computed time/frequency plot of experimental 80-kHz Chirp*

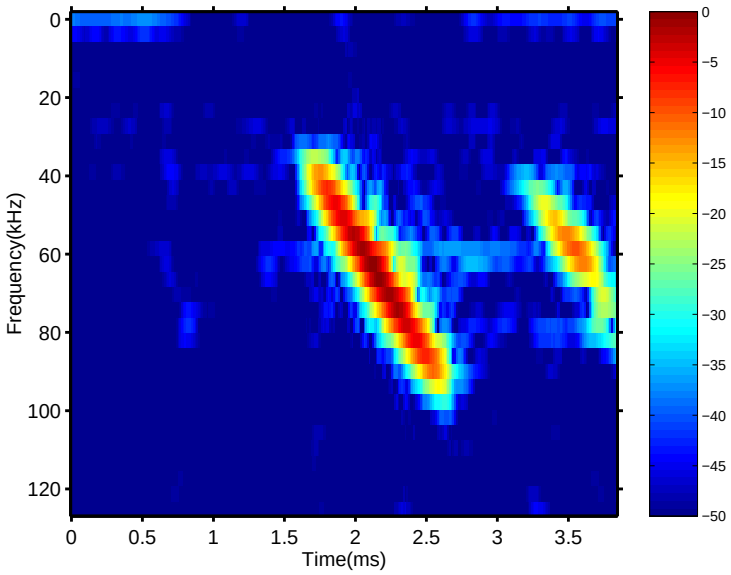

Figure 23: *Computed time/frequency plot of experimental 60-kHz Chirp*

matched filter time series and its Hilbert transform) when we cross-correlate the recorded time series with the theoretical input pulses for the 5 pulse sequence of Gaussian pulses, first when the individual pulses are separated by 80 μseconds and by 40 μseconds. A very good time compression has resulted for both cases. In Fig. 28 we show the results of match filtering the recorded time series produced with the 11 bit Barker Code 62.5 kHz cosine pulse with the desired pulse sequence. Once again, a very good time compression has been achieved. In these matched filtered time series the second peak corresponds to the surface-reflected arrival. As discussed previously, due to the vertical azimuthal dependence of the transducer frequency response, the surface reflection does not cross-correlate as well as the direct arrival with the incident pulse. The frequency compensation which works well for the small vertical angles angles is not correct for energy at higher vertical angles.

As another example of this we consider the time series for the 80 kHz Chirp. In this case, the receiver and transducer were moved to approximately 3 feet below the water surface. In this case the pulses from the direct and surface reflected paths overlap. As well, there are other reflections from the back and sides of the tank. Also, a small aluminum sphere (air-filled) (shown in Fig.29) was placed behind the receiver. The echo from this sphere is weak. In Fig.30 the original time series is shown. The incident and surface reflected pulse overlap with each. The echo from the sphere can not be identified.

The results of match-filtering the time series with the theoretical Chirp pulse is shown in Fig. 31 (here we simply show the matched filter results and not

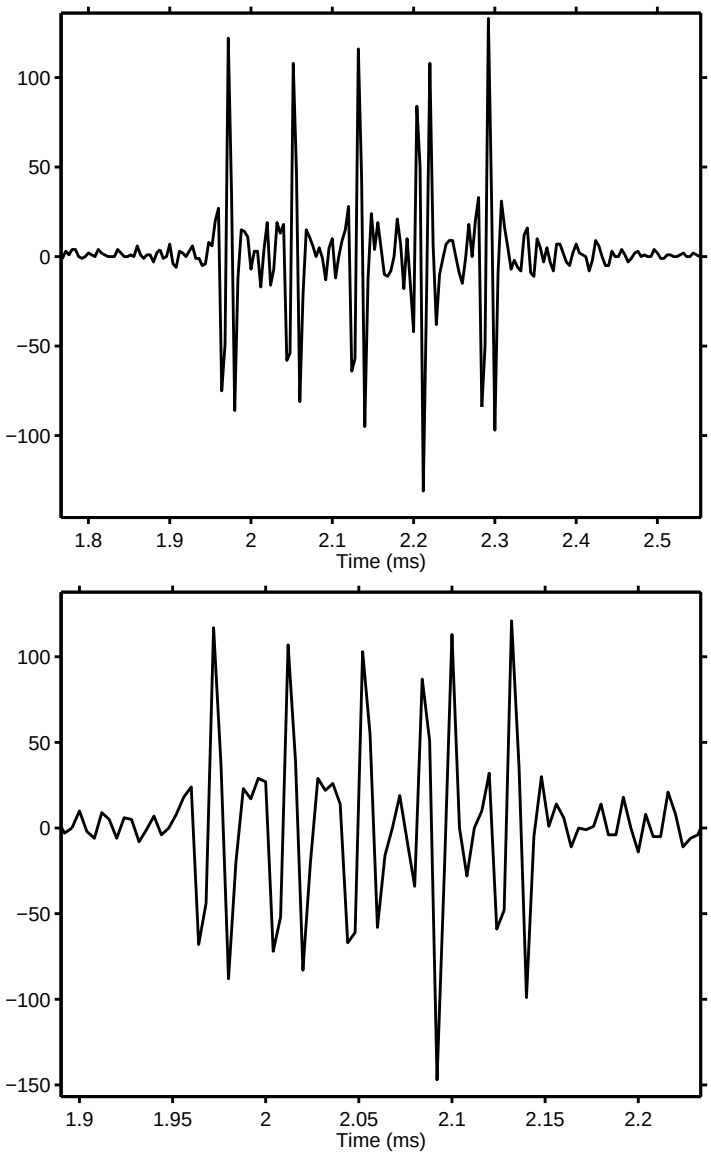

Figure 24: *A 5 pulse Barker sequence using individual Gaussian pulses with a separation of 20 samples (80 μsecs) between pulses and 10 samples (40 μsecs) between pulses)*

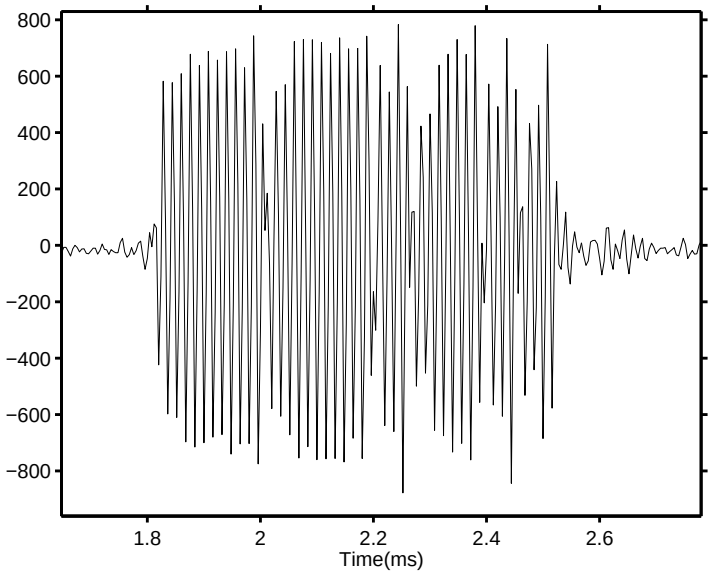

Figure 25: *A 11 pulse Barker sequence using a cosine carrier at 62.5 kHz*

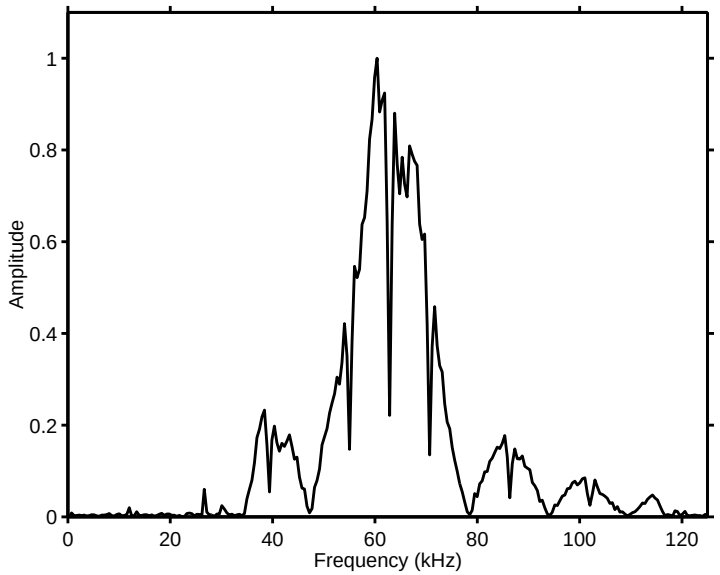

Figure 26: *The spectrum of the Barker code time series of Fig. 25*

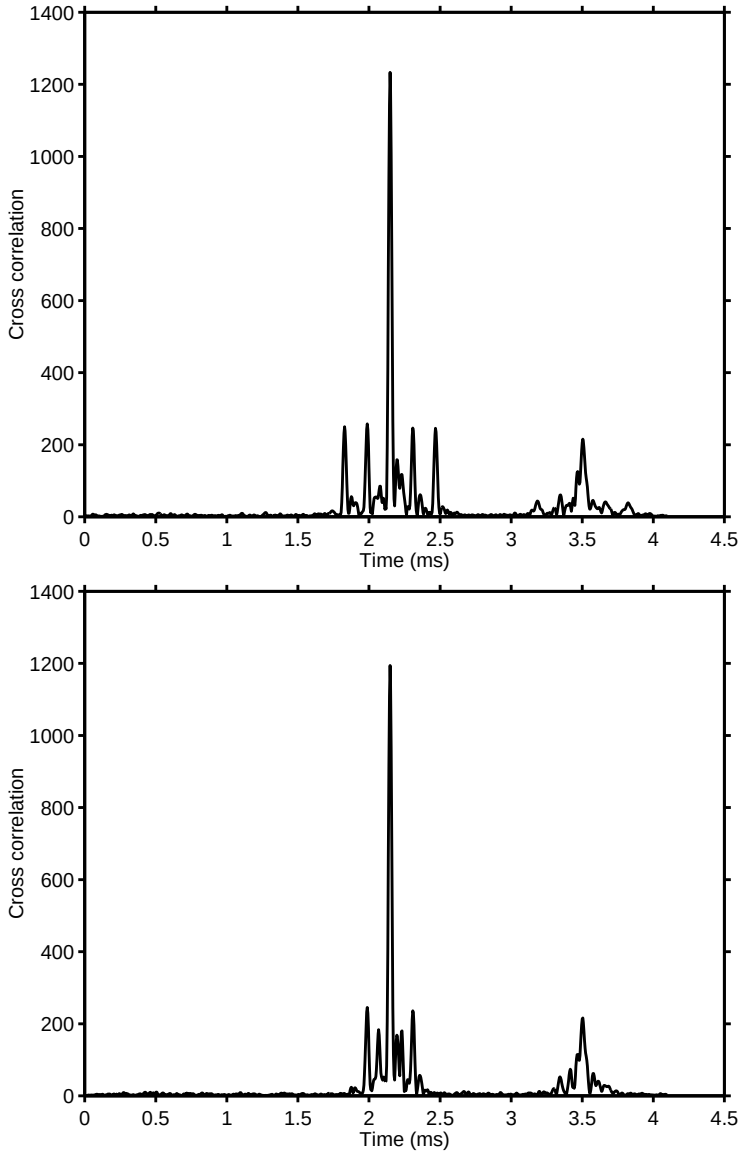

Figure 27: *The matched filter time series using the Barker code of individual Gaussian pulses separated by 80 μsecs and 40 μsecs respectively)*

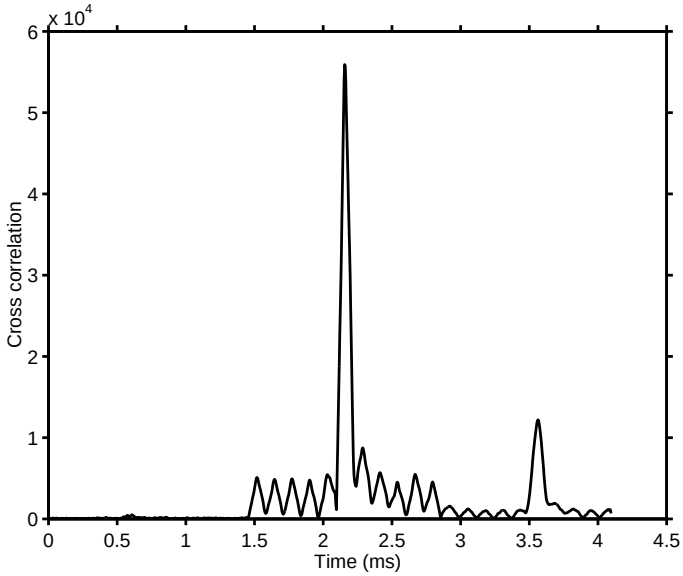

Figure 28: *The matched filter time series from the 11 Barker code using a 62.5 kHz cosine burst.*

Figure 29: *The small aluminum-shelled sphere that was deployed in tank*

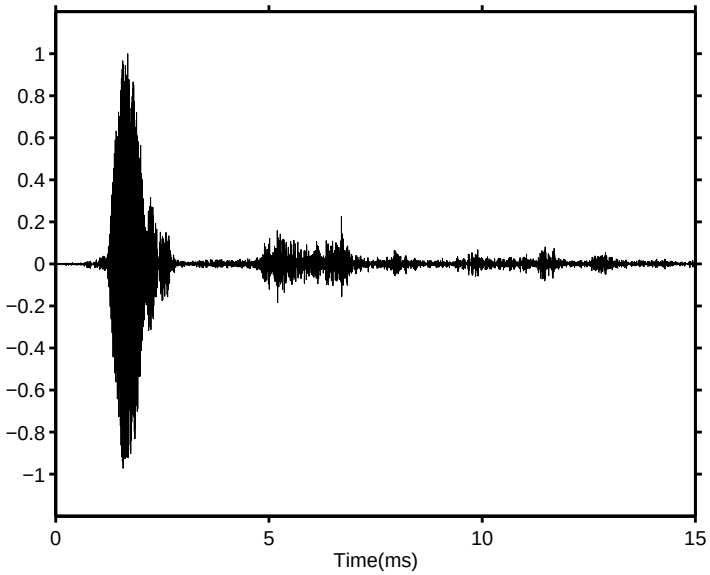

Figure 30: *The timeseries with overlapping incident and multipath pulses.*

the amplitude of the complex envelope) and a zoom of the region near the sphere echo is shown. Although, the echo is relatively weak it is certainly detectable in the matched filtered time series. This echo sequence contains the specular reflection and other reflections, possibly from the flange as well as circumferential arrivals.

The matched filtering results are consistent with those predicted by theory. For example, the width of the main lobe for the 11-term Barker code (using the 62.5 kHz burst) is approximately 132 μ seconds which corresponds to an effective bandwidth of approximately 15 kHz, which is consistent with the spectrum of Fig. 26. When using the 80-kHz Chirp, the width of the main matched-filter lobe is 40 μ seconds corresponding to an effective bandwidth of 50 kHz, which is also consistent with the spectrum of the the pulse (even though we used 80 kHz in the definition of the Chirp, the effective bandwidth is less due to the properties of the Chirp and the cosine weighting applied). Also, as illustrated with the echo time series from the sphere, the use of the matched filtering has improved the signal-to-noise ratio from the original time series.

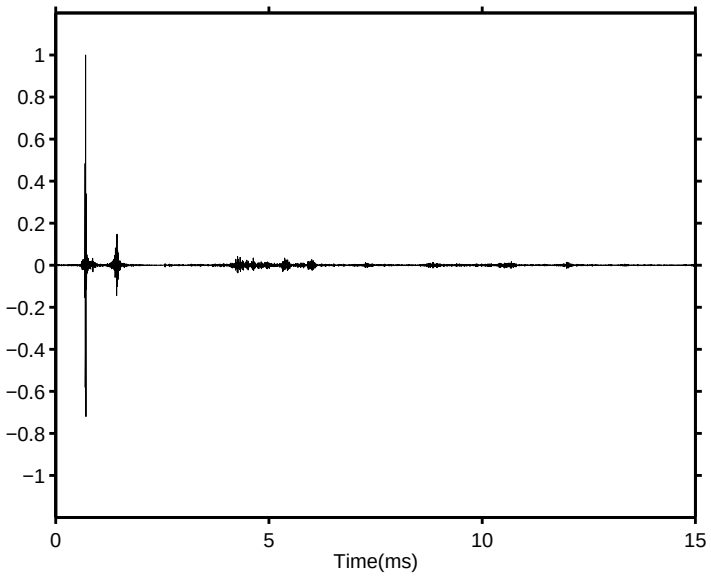

Figure 31: *The matched filtered version of the time series of Fig. 30*

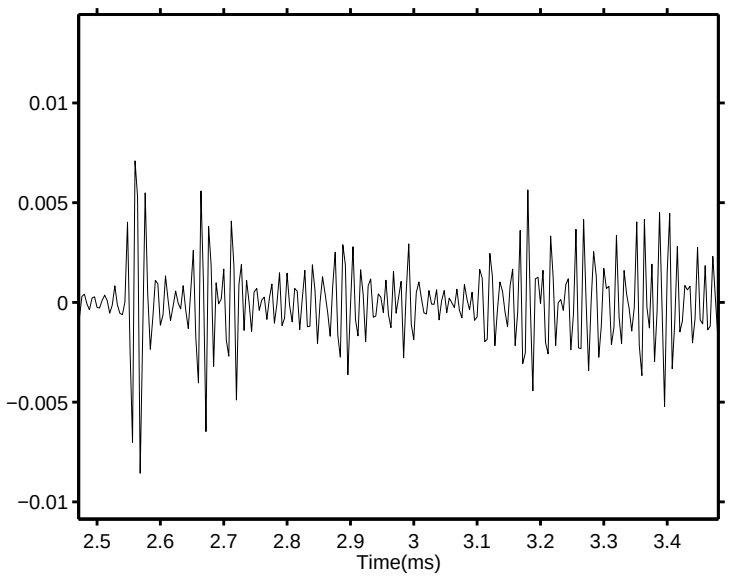

Figure 32: *The matched filtered version of the time series of Fig. 30, zoomed in near the region of the sphere echo*

3 VERTICAL BEAMPATTERN

In the data presented so far, even for the 2 element MMPP arrays, the sonar was deployed with the axis of symmetry vertically. For example, for a single MMPP the middle slot would be oriented in a horizontal plane. The horizontal beampattern should be approximately omnidirectional. The vertical beampattern, however, will be much more complicated. To measure this vertical beampattern, the MMPP was held horizontally and then rotated in an uniform fashion. The FFT spectrum of the recorded signal for a 80-kHz wide incident pulse (noncompensated) is shown in Fig.33 as a function of the rotation angle. It is clear from this plot there is significant energy from the circular endcaps (approximately 60° and 240° in the plot) of the transducer and this region is relatively broad. The spectra which we have been examining in this paper correspond to the broadside direction (approximately 150° and 330°). It can be seen that the beamwidth of this broadside energy is quite narrow, particularly at the higher frequencies. This would mean that in its vertical orientation there would be an omni-direction horizontal beam and a narrow vertical beamwidth. On the other hand, if the transducer is oriented horizontally, there is an omnidirectional vertical beampattern and a very narrow horizontal beam pattern. It is also clear that the endfire directions which would have a fairly broad conical beam could also be useful. The null at approximately 30 kHz for the broadside direction appears to be somewhat less for the endfire direction.

In Fig. 34 we use the compensated 80-kHz Sinc waveform and consider the vertical beampattern measurement in this case. The compensation has been successful for the broadside direction but has not compensated the other directions correctly. In fact, the relative amplitude of the signal from the endfire direction appears to be somewhat higher now (as compared to the case of the uncompensated spectra). Finally, in Figs.35 and 36 we show the recorded time series and corresponding spectrum for a compensated Sinc pulse (20-70 kHz) with the transducer's flat circular endcap facing the hydrophone. Here the spectrum $S(f)$ used in Eq.(5) was that for the endfire direction. As can be seen, the compensation for the endfire orientation has been very successful.

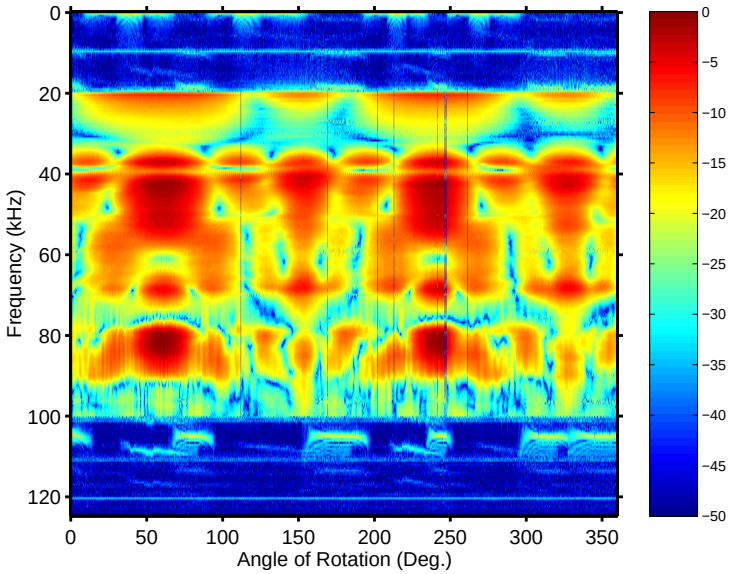

Figure 33: *The vertical beampattern of the transducer for an uncompensated 80-kHz Sinc waveform*

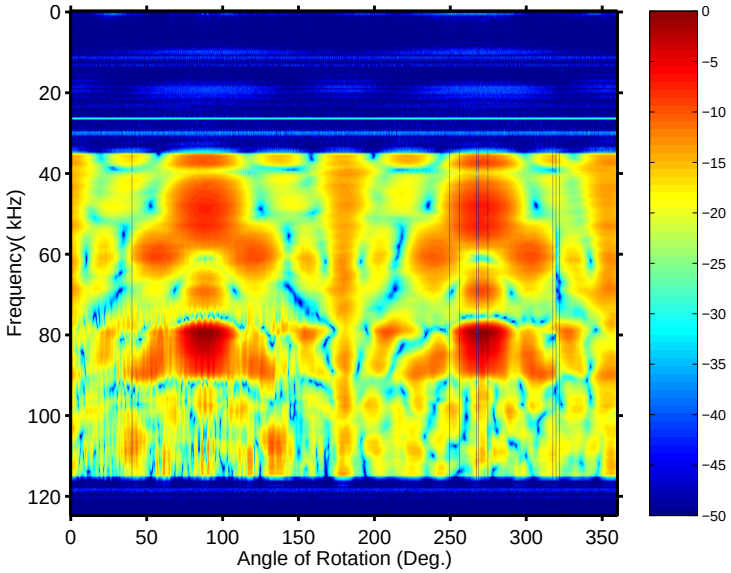

Figure 34: *The vertical beampattern of the transducer for a compensated 80-kHz Sinc waveform for the broadside direction*

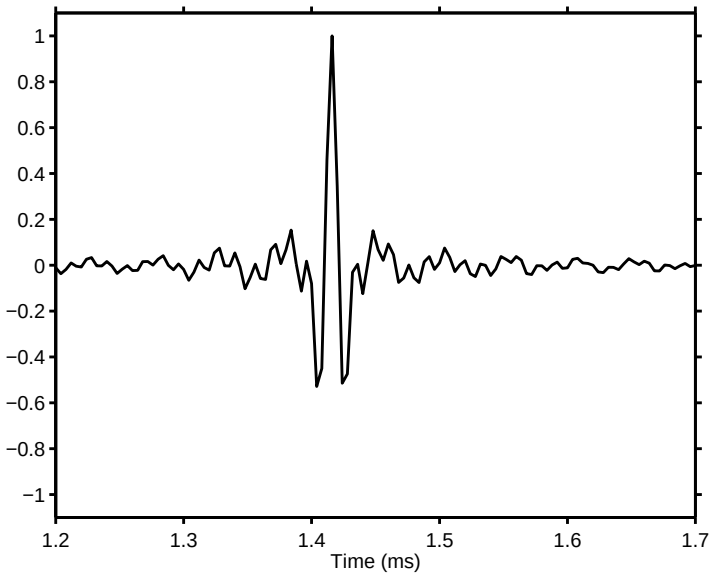

Figure 35: *Time series using compensated Sinc pulse (20-70 kHz) for transducer endcap facing hydrophone*

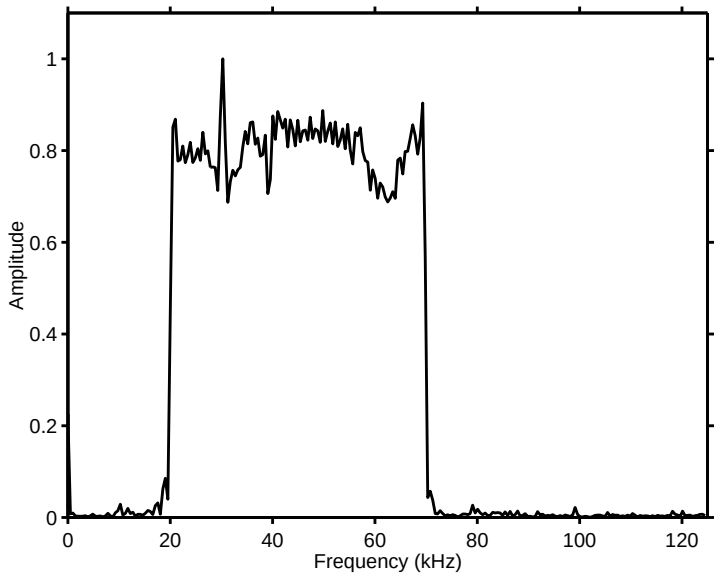

Figure 36: *The power spectrum of the resultant signal*

4 DISCUSSION OF RESULTS

In this report it has been shown the high frequency MMPP has a very wideband response. The spectral response of the transducer can be simply compensated for in order to produce specified wideband pulses, either very impulsive or extended in time in the case of 1 millisecond Chirp pulses. Additionally, pulse sequences can be created by amplitude modulating individual pulse types. As an example of these pulse sequences, we used Barker code sequences for the amplitudes. It was shown that by match filtering the signals recorded at the hydrophone with the ideal (before compensation) waveform, either a pulse sequence or a Chirp, very precise arrival times (i.e., very time compressed outputs) with small sidelobe levels were obtained. Thus the high frequency MMPP shows good potential for the production of specified pulses in the frequency band 35-115 kHz (for the standard vertical orientation).

The vertical beampattern of the transducer was also investigated. It was found that frequency/azimuthal dependence of the transducer is rather complicated. In this report we have emphasized the on-axis response of the transducer with the endcaps oriented vertically. The vertical beampattern measurements indicate that in this orientation the transducer has quite a narrow vertical beampattern and an almost omni-directional horizontal beampattern (from the azimuthal symmetry of the transducer). For applications where a broad vertical beampattern and a narrow horizontal beampattern are required, these characteristics can be obtained by orienting the transducer with the endcaps horizontal and the centre slot facing the hydrophone. It is also seen from the vertical beampattern measurements that the compensating spectrum used for the on-axis energy is not correct for angles sufficiently away from this direction, particularly at the higher frequencies. There are advantages to orienting the transducer so that one of the endcaps is facing the receiver. This orientation seems to provide more power and its beampattern is conical in nature. The null at 30 kHz is relatively less than for the broadside orientation and a 20-70 kHz Sinc pulse was very accurately produced for this orientation. The beampattern is broader for this orientation and thus the computed compensating spectrum should be valid over a larger range of angles.

It should be possible, due to their small size, to construct an array of these high frequency MMPP sources. The overall frequency and beampattern characteristics of the resulting system will depend upon the coupling between the transducers, the wiring (e.g., in phase or out-of-phase) of the transducers and the inter-element spacing.

In the future it is hoped to investigate the performance of all sizes of the MMPP in longer-range sea experiments. It is hoped that a prototype wideband sonar system consisting of possibly an array of sources and an array of receiver elements can be constructed.

References

1. C.J. Purcell, C. J. and R. Fleming, *Multi-Mode Pipe Projector*, US Patent 6,584,039 (2003)

2. R. Fleming, "High frequency multi-mode pipe projector", DRDC-Atlantic TM 2003-218, November 2003

3. M. Trevorrow and D. Farmer, "The use of Barker Codes in Doppler sonar measurements", Journal of Atmospheric and Oceanic Technology, Vol.9, No.5, October 1992.

Distribution List

Internal Distribution

David Hopkin,
Mine and Torpedo Defence Group,
9 Grove St.,
Dartmouth, Nova Scotia, B2Y 3Z7

Mark Trevorrow,
Mine and Torpedo Defence Group,
9 Grove St.,
Dartmouth, Nova Scotia, B2Y 3Z7

Anna Crawford,
Mine and Torpedo Defence Group,
9 Grove St.,
Dartmouth, Nova Scotia, B2Y 3Z7

Terry Miller,
Mine and Torpedo Defence Group,
9 Grove St.,
Dartmouth, Nova Scotia, B2Y 3Z7

Juri Sildam,
Mine and Torpedo Defence Group,
9 Grove St.,
Dartmouth,Nova Scotia, B2Y 3Z7

John Fawcett,
Mine and Torpedo Defence Group,
9 Grove St.,
Dartmouth,Nova Scotia, B2Y 3Z7

Art Collier,
Mine and Torpedo Defence Group,
9 Grove St.,
Dartmouth,Nova Scotia, B2Y 3Z7

Chris Purcell,
Sensors and Actuators Group,
9 Grove St.,
Dartmouth,Nova Scotia, B2Y 3Z7

Garry Heard,
Rapidly Deployable Systems Group,
9 Grove St.,
Dartmouth,Nova Scotia, B2Y 3Z7

Brian Maranda,
Sonar Signal Processing Group,
9 Grove St.,
Dartmouth,Nova Scotia, B2Y 3Z7

Library (5)

External Distribution

NDHQ/DRDKIM

DOCUMENT CONTROL DATA

(Security classification of title, body of abstract and indexing annotation must be entered when the overall document is classified)

1. ORIGINATOR (the name and address of the organization preparing the document. Organizations for whom the document was prepared, e.g. Centre sponsoring a contractor's report, or tasking agency, are entered in section 8.)

Defence R&D Canada – Atlantic, PO Box 1012, Dartmouth, NS B2Y 3Z7

2. SECURITY CLASSIFICATION (overall security classification of the document including special warning terms if applicable).

UNCLASSIFIED

3. TITLE (the complete document title as indicated on the title page. Its classification should be indicated by the appropriate abbreviation (S,C,R or U) in parentheses after the title).

Broadband pulse synthesis with the high frequency Multi-Mode Pipe Projector

4. AUTHORS (Last name, first name, middle initial. If military, show rank, e.g. Doe, Maj. John E.)

John Fawcett, Juri Sildam, Terry Miller, Richard Fleming, and Mark Trevorrow

5. DATE OF PUBLICATION (month and year of publication of document)

April 2005

6a. NO. OF PAGES (total containing information Include Annexes, Appendices, etc).

32 (approx.)

6b. NO. OF REFS (total cited in document)

3

7. DESCRIPTIVE NOTES (the category of the document, e.g. technical report, technical note or memorandum. If appropriate, enter the type of report, e.g. interim, progress, summary, annual or final. Give the inclusive dates when a specific reporting period is covered).

Technical Memorandum

8. SPONSORING ACTIVITY (the name of the department project office or laboratory sponsoring the research and development. Include address).

Defence R&D Canada – Atlantic
PO Box 1012
Dartmouth, NS, Canada B2Y 3Z7

9a. PROJECT OR GRANT NO. (if appropriate, the applicable research and development project or grant number under which the document was written. Please specify whether project or grant).

11CY04

9b. CONTRACT NO. (if appropriate, the applicable number under which the document was written).

10a ORIGINATOR'S DOCUMENT NUMBER (the official document number by which the document is identified by the originating activity. This number must be unique to this document.)

DRDC Atlantic TM 2005-022

10b OTHER DOCUMENT NOs. (Any other numbers which may be assigned this document either by the originator or by the sponsor.)

11. DOCUMENT AVAILABILITY (any limitations on further dissemination of the document, other than those imposed by security classification)

(X) Unlimited distribution
( ) Defence departments and defence contractors; further distribution only as approved
( ) Defence departments and Canadian defence contractors; further distribution only as approved
( ) Government departments and agencies; further distribution only as approved
( ) Defence departments; further distribution only as approved
( ) Other (please specify)

12. DOCUMENT ANNOUNCEMENT (any limitation to the bibliographic announcement of this document. This will normally correspond to the Document Availability (11). However, where further distribution (beyond the audience specified in (11) is possible, a wider announcement audience may be selected).

13. ABSTRACT (a brief and factual summary of the document. It may also appear elsewhere in the body of the document itself. It is highly desirable that the abstract of classified documents be unclassified. Each paragraph of the abstract shall begin with an indication of the security classification of the information in the paragraph (unless the document itself is unclassified) represented as (S), (C), (R), or (U). It is not necessary to include here abstracts in both official languages unless the text is bilingual).

In this report we describe experiments carried out at the DRDC Atlantic tank facility with the high frequency broadband Multi-Mode Pipe Projector (MMPP). In particular, we examine the fidelity with which one can produce specified broadband pulses with and without compensation for the transducer's spectral characteristics. It is shown that extended pulses or pulse sequences can be accurately produced and that matched filtering very effectively compresses the time series in the case of extended pulses. In addition, the vertical beampattern of the transducers is discussed and the results of some experiments with 2 transducers are also presented.

14. KEYWORDS, DESCRIPTORS or IDENTIFIERS (technically meaningful terms or short phrases that characterize a document and could be helpful in cataloguing the document. They should be selected so that no security classification is required. Identifiers, such as equipment model designation, trade name, military project code name, geographic location may also be included. If possible keywords should be selected from a published thesaurus. e.g. Thesaurus of Engineering and Scientific Terms (TEST) and that thesaurus-identified. If it not possible to select indexing terms which are Unclassified, the classification of each should be indicated as with the title).

broadband, matched filtering, transducer

This page intentionally left blank.

Defence R&D Canada

Canada's leader in defence
and National Security
Science and Technology

R & D pour la défense Canada

Chef de file au Canada en matière
de science et de technologie pour
la défense et la sécurité nationale

DEFENCE DÉFENSE

www.drdc-rddc.gc.ca